View metadata, citation and similar papers at core.ac.uk
brought to you by CORE
provided by Repositorio Institucional de la Universidad de Alicante

JAAS
FULL PAPER
www.rsc.org/jaas

# The role of the nebulizer on the sodium interferent effects in inductively coupled plasma atomic emission spectrometry

**Jesús M. Cano, José L. Todolí, Vicente Hernandis and Juan Mora***

*Departamento de Química Analítica, Universidad de Alicante, P.O. Box 99, 03080 Alicante, Spain. E-mail: juan.mora@ua.es*

***Received 11th June 2001, Accepted 6th November 2001***
***First published as an Advance Article on the web 3rd December 2001***

The role of the nebulizer on the sodium chloride interferent effects in ICP-AES was investigated. Three different pneumatic nebulizers coupled to a cyclonic spray chamber were investigated: a V-groove (VGN) and two new pneumatic concentric nebulizers specifically designed to work with saline solutions (the 'Seaspray' nebulizer, SSN, and experimental nebulizer, EN). The effect of the salt concentration on the characteristics of the aerosols generated by the nebulizers (primary aerosols) and those at the exit of the spray chamber (tertiary aerosols) on the transport parameters and on the analytical figures of merit in ICP-AES were evaluated. The characteristics of the primary aerosols were related to their critical dimensions and were independent of the solution salt concentration. Solvent and analyte transport rates were related to the characteristics of the primary aerosols. Thus, the SSN provided the highest solution transport rates followed by the EN and VGN. The Mn II emission signal correlated quite well with transport parameters. When the salt concentration increased, an interference effect on the ICP-AES emission signal was observed. This effect was related to the nebulizer employed. Thus, for the SSN, the effect of the sodium chloride on the emission signal was different for the ionic and atomic lines. For the remaining nebulizers, a depressive effect of the salt concentration on the emission signal was always observed irrespective of the line considered. The magnitude of the interference was different for each nebulizer and was related to the amount of solvent transported to the plasma. In general terms, by increasing the salt concentration, poorer signal precision and limits of detection were obtained. These results confirm the importance of sustaining robust plasma conditions to reduce the sodium chloride interferences.

## Introduction

One of the most important goals in quantitative analysis is to have an analytical method that is as independent as possible of the sample matrix. To overcome matrix interferences, a clear understanding of their effects is required. In inductively coupled plasma atomic emission spectrometry (ICP-AES) the most common matrices are those containing the so-called easily ionized elements (EIE) and acids. Both matrices have certainly been the most studied in terms of interferences in ICP-AES.[1–7]

The effect of EIE in ICP-AES is quite complex. In general terms, interferences can arise from: (i) changes in the amount of aerosol introduced into the plasma; and, (ii) changes in the plasma excitation conditions. The former are directly related to the sample introduction system. The latter can be related to the plasma experimental conditions (*i.e.*, rf power, gas flows, *etc*).

A conventional liquid sample introduction system in ICP-AES consists of a nebulizer, usually pneumatic concentric, coupled to a spray chamber. Sometimes a desolvation system is also included to reduce the amount of solvent introduced into the atomization/excitation cell. Thus, interferences due to the presence of solvent in the plasma can be avoided or, at least, reduced. The effect of the spray chamber on the acid- and the EIE interferences in ICP-AES has been thoroughly studied.[8–11] Nevertheless, little evidence about the role of the nebulizer on the EIE effects has been found in the literature. Several reasons can be found to explain this fact. Among them, the risk of clogging of the conventional pneumatic concentric nebulizers when working with high salt content solutions must be considered. To overcome this drawback, different nebulizers have been developed.[12] Most of them are of a pneumatic nature, based either on the Babington principle,[13–15] such as the V-groove,[14] the conespray[16] and the Hildebrand grid nebulizers,[15] or on modifications of the conventional concentric nebulizers.[15,17] Unfortunately, these nebulizers usually give rise to poorer analytical figures of merit than the conventional ones. To overcome this problem, several highly efficient nebulizers have been proposed. Among them, nebulizers such as the single-bore high-pressure pneumatic nebulizer[18] or the microwave-based thermal nebulizer[19] are good alternatives to the conventional pneumatic ones to operate with high salt content solutions. The main problem of these nebulizers is the requirement of a desolvation system, due to the high amount of solvent transported to the plasma.

The purpose of the present work is to provide evidence of the role of the sample introduction system, mainly the nebulizer, in the analysis of high salt (sodium chloride) content solutions by ICP-AES. To this end, two new pneumatic concentric nebulizers and a V-groove nebulizer have been used. The effect of the salt concentration on the characteristics of the aerosols generated, on the transport parameters and on the analytical figures of merit in ICP-AES has been evaluated.

## Experimental

### Reagents and samples

Test solutions containing 1 μg ml$^{-1}$ of each element were prepared by dilution of a 1000 μg ml$^{-1}$ multi-elemental reference solution (IV, Merck, Darmstadt, Germany) with solutions of different NaCl concentration. Table 1 shows the physical properties of the solutions tested. Density was directly obtained by weighing a given volume of each solution. For the viscosity measurements, a Cannon-Fenske type viscometer (Selecta, Barcelona, Spain) was used. Surface tension values were obtained by using the drop weight method.[20]



**This journal is © The Royal Society of Chemistry 2002**

**Table 1** Physical properties of the solutions tested

| NaCl concentration (%) | Density/ g mL$^{-1}$ | Viscosity/ cP | Surface tension/dyn cm$^{-1}$ |
|---|---|---|---|
| 0 | 1.000 | 1.00 | 70.43 |
| 2 | 1.014 | 1.00 | 71.24 |
| 4 | 1.028 | 1.02 | 71.94 |
| 6 | 1.042 | 1.01 | 72.42 |
| 8 | 1.056 | 1.05 | 72.96 |
| 10 | 1.070 | 1.08 | 73.60 |

### Sample introduction system

Two pneumatic concentric nebulizers specifically designed to work with high salt content solutions, the 'Seaspray' nebulizer, SSN, and 'experimental' nebulizer, EN (Glass Expansion, Victoria, Australia) were used. The last is a prototype designed to work with both high salt content solutions and slurries. A V-Groove nebulizer, VGN (Varian, Australia), usually employed with high salt content solutions[14] was used for comparison. For the fundamental studies on aerosol characteristics, three extra pneumatic concentric nebulizers were tested: a 'Conikal' nebulizer, CN (Glass Expansion, Victoria, Australia), an A-type concentric nebulizer, AN (Model TR-30-A3, Meinhard, Santa Ana, CA, USA), and a nebulizer designed to work with slurries, the so called 'slurry' nebulizer, SN (Glass Expansion, Victoria, Australia). Fig. 1 and Table 2 show the scheme and dimensions, respectively, of the nebulizers used.

A polypropylene cyclonic-type spray chamber (Glass Expansion, Victoria, Australia) with a 62 mL inner volume was used in all cases. This spray chamber was selected since it shows lower matrix effects than the conventional double pass one.[8] Thus, the role of the nebulizer on the analytical response will be highlighted.

Sample uptake rate ($Q_l$) to the nebulizer was controlled by means of a peristaltic pump (Model Minipulse 3, Gilson, Villiers-Le-Bel, France). The nebulizer gas flow rate ($Q_g$) was controlled by means of a mass flow controller (Model FC-260, Tylan, Torrance, CA, USA). Argon was always used as the nebulizer gas.

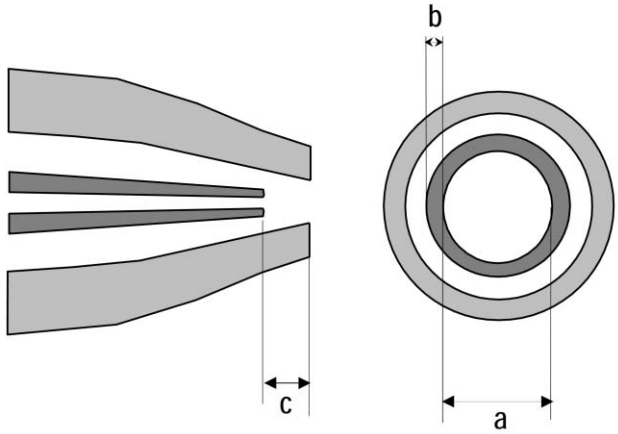


**Fig. 1** Scheme of the pneumatic concentric nebulizers used: a, liquid capillary inner diameter; b, liquid capillary wall thickness; c, distance between the outlets of liquid and gas streams.

**Table 2** Critical dimensions (see Fig. 1 for explanation) and nebulization yields of the nebulizers tested

| Nebulizer | $a^a$/mm | $b^b$/mm | $c^c$/mm | $A_g^d/\times 10^2$ mm$^2$ | Aerosol yield (%) |
|---|---|---|---|---|---|
| SSN | 0.22 | 0.05 | 0.80 | 1.45 | 100 |
| EN | 0.40 | 0.04 | 1.20 | 1.04 | 43 |
| CN | 0.20 | 0.10 | 0.92 | 1.50 | 100 |
| AN | 0.40 | 0.06 | 0 | 2.8 | 100 |
| SN | 0.52 | 0.03 | 1.32 | 1.41 | 32 |
| VGN | — | — | — | 1.16 | 100 |

[a]Liquid capillary inner diameter. [b]Liquid capillary wall thickness. [c]Distance between liquid capillary and gas outlets. [d]Effective gas outlet section area.

### Aerosol drop size distribution measurements

Drop size distributions (DSD) of the aerosols were measured by means of a laser Fraunhofer diffraction system (Model 2600c, Malvern Instruments Ltd., Malvern, Worcestershire, UK). The software employed was version B.0D. All measurements were made downstream at a distance of 6 mm from the nebulizer tip, or from the exit of the spray chamber for the primary and tertiary aerosols, respectively. A lens with focal length of 63 mm, which enables the system to measure droplets with diameters between 1.2 and 118 μm, was used. The calculations to transform the energy distribution into size distribution were made using a model-independent algorithm that does not preclude any particular distribution function. A set of five replicates was performed in each case; the relative standard deviation of these measurements was always lower than 2%.

### Transport measurements

Solvent and analyte transport measurements were performed by means of direct methods. Solvent transport rate ($S_{tot}$) was measured by the adsorption of the aerosol in a U-tube filled with silica gel during a 10 min period. By weighing the U-tube before and after the aerosol exposure, the $S_{tot}$ values can be easily obtained. Analyte transport rates ($W_{tot}$) were obtained by collecting the aerosol on a glass fibre filter (type A/E, 47 mm diameter, 0.3 μm pore size, Gelman Sciences, USA) placed above the spray chamber. A 500 μg mL$^{-1}$ Mn solution was nebulized. The analyte retained after a period of time (10 min) was extracted by washing the filters with a 1.0% (w/w) nitric acid solution. After that, the total solution mass was made up to 30 g. Finally, the Mn concentration in each solution was determined by flame atomic absorption spectrometry. A set of three replicates was performed in each case and the precision of these measurements was always better than 5%.

### ICP-AES instrumentation

A Perkin-Elmer Optima 3000 ICP-AES system (Perkin-Elmer, Uberlingen, Germany) was used for the measurements of emission signal data. Table 3 shows the experimental conditions used.

Several atomic lines covering a range of excitation energies, $E_{exc}$, from 3.14 eV (Al I 396.152) to 5.80 eV (Zn I 213.856) were used. Ionic lines were selected to cover a range of energy sum values, $E_{sum}$, (*i.e.*, sum of the ionization, $E_{ion}$, and excitation energies) from 7.93 eV (Ba II 455.403) to 14.79 eV (Pb II 220.353). Table 4 shows the wavelengths and energies of the lines tested.

**Table 3** ICP-AES conditions

| | |
|---|---|
| Rf power/kW | 1.3 |
| Outer gas flow/L min$^{-1}$ | 15 |
| Intermediate gas flow/L min$^{-1}$ | 0.5 |
| Nebulizer gas flow/L min$^{-1a}$ | 0.5 |
| View height ALC/mm | 7 |
| Integration time/s | 0.1 |
| Uptake rate/mL min$^{-1}$ | 1.0 |

[a]Optimum value for all the nebulizers tested.

**Table 4** Energy values for the selected lines

| Element | Wavelength/nm | $E_{exc}$/eV | $E_{ion}$/eV | $E_{sum}$[a]/eV |
|---|---|---|---|---|
| Al I | 396.152 | 3.14 | | 3.14 |
| Cr I | 357.869 | 3.46 | | 3.46 |
| Cu I | 324.754 | 3.82 | | 3.82 |
| Mg I | 285.213 | 4.35 | | 4.35 |
| Zn I | 213.856 | 5.80 | | 5.80 |
| Ba II | 455.403 | 5.21 | 2.72 | 7.93 |
| Sr II | 407.771 | 3.04 | 5.69 | 8.73 |
| Mg II | 280.270 | 7.65 | 4.42 | 12.07 |
| Mn II | 257.610 | 7.44 | 4.81 | 12.25 |
| Cr II | 205.560 | 6.77 | 6.03 | 12.80 |
| Cr II | 267.716 | 6.77 | 6.16 | 12.92 |
| Fe II | 238.204 | 5.20 | 7.87 | 13.07 |
| Co II | 228.616 | 7.86 | 5.84 | 13.70 |
| Ni II | 221.647 | 7.64 | 6.39 | 14.03 |
| Cd II | 214.438 | 5.78 | 8.99 | 14.77 |
| Pb II | 220.353 | 7.42 | 7.37 | 14.79 |

[a] $E_{sum}$ = ionization energy ($E_{ion}$) + excitation energy ($E_{exc}$).

### Statistical calculations

Cluster analysis was carried out by applying the Ward method for agglomeration, with the square of the Euclidean distance as a criterion of proximity. This analysis was performed using the Statistical Package of Social Science, version 10.0 software (SPSS Inc., Chicago, IL, USA).

## Results and discussion

Two factors determine the analytical ICP signal: (i) the amount of analyte reaching the plasma per time unit (*i.e.*, the analyte transport rate, $W_{tot}$), which depends on the characteristics of the aerosols generated by the nebulizer (*i.e.*, primary aerosols) and on the transport phenomena that occur during its transport to the plasma through the spray chamber; and (ii) the fraction of the excited analyte within the observation volume of the plasma, which is influenced by, in addition to the analyte and solvent transport rates ($W_{tot}$ and $S_{tot}$, respectively), the characteristics of the aerosol reaching the plasma (*i.e.*, tertiary aerosol) and by plasma robustness. All these factors strongly depend on the sample (solution) composition.

### Characteristics of the primary aerosols

**Primary aerosol drop size distribution.** Fig. 2 shows the variation of the Sauter mean diameter of the primary aerosols ($pD_{3,2}$) *versus* the sodium concentration of the solution for all the nebulizers studied. From these results it can be seen that, irrespective of the nebulizer tested, the presence of sodium scarcely affects the $pD_{3,2}$ values. Data shown in Table 1 support this behaviour, since the presence of sodium chloride hardly affects the surface tension or the viscosity of the solution. Therefore, no relevant differences in the primary DSD (pDSD) are expected.[16,21]

Both the SSN and the EN are capable of continuous operation with concentrated sodium chloride solutions without any of the clogging problems typically observed with the conventional pneumatic concentric nebulizers. It has been claimed that the distance between the liquid capillary and the nebulizer tip (c, in Fig. 1 and Table 2) enables the concentric nebulizers to operate with high salt content solutions.[22]

Regarding the relative behaviour of the nebulizers evaluated, Fig. 2 shows that, for all the solutions tested, the finest primary aerosols are obtained with the SSN and the coarsest with the EN. This behaviour can be explained in relation to the main dimensions of the nebulizers.[16,23] Firstly, the gas outlet section area ($A_g$) determines the amount of kinetic energy available for the aerosol generation. Thus, for a given $Q_g$, the energy of the gas stream increases as $A_g$ decreases (increased pressure required). Therefore, the capability of generating a new surface is also increased with the result of finer aerosols. Secondly, the liquid capillary inner diameter and its wall thickness (a and b in Fig. 1, respectively) influence the effectiveness of the energy transference process to the liquid bulk. For a given amount of energy, the smaller the dimensions of these parameters, the higher is the effectiveness of the process and, therefore, the finer the aerosols generated. Among the concentric nebulizers tested, the SSN shows the highest $A_g$ (Table 2). Therefore, by just considering this parameter, the SSN should produce the coarsest primary aerosols. Nevertheless, the lowest value of the capillary inner diameter (Table 2) counterbalances this factor and, as a result, the SSN is the nebulizer that generates the aerosols with the lowest $pD_{3,2}$ values (Fig. 2).

**Nebulization yield.** In addition to the pDSD, some other parameters must be considered to fully describe the characteristics of the primary aerosols. One of these characteristics is the nebulization yield, *i.e.*, the fraction of the pumped sample mass that is transformed into an aerosol.

Table 2 shows the aerosol yields obtained for all the nebulizers tested. It can be observed that, among the three nebulizers studied (SSN, EN and VGN), only the EN gives rise to nebulization yields lower than 100%. Under the nebulization conditions listed in Table 3, the EN transforms only 43% of the solution into an aerosol. The rest of the solution is lost at the nebulizer tip (see Fig. 3). This behaviour must be related, for given experimental conditions, to the main dimensions of the concentric nebulizer, *i.e.*, gas outlet section area ($A_g$), liquid capillary inner diameter ($a$) and wall thickness ($b$), and the recessed area of the liquid capillary with respect to the nebulizer tip (c). To provide evidence for this fact, five pneumatic concentric nebulizers with different critical dimensions were used and the aerosol yields measured (Table 2). As can be seen in Table 2, the EN and SN give rise to aerosol yields

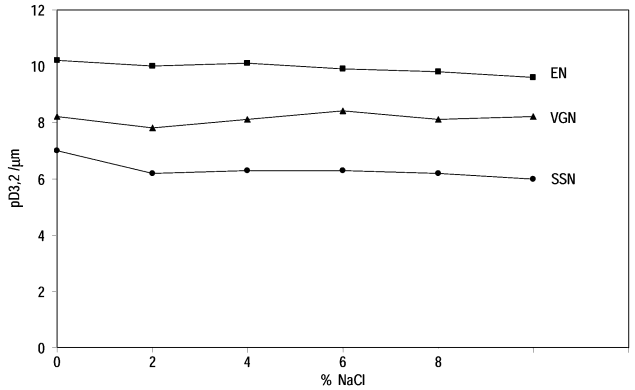


**Fig. 2** Effect of the sodium chloride concentration on the Sauter mean diameter of the primary aerosol, $pD_{3,2}$, for all the nebulizers tested.

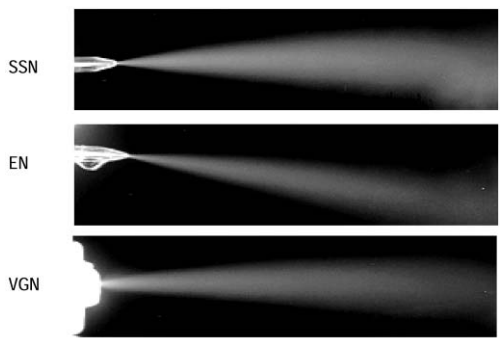


**Fig. 3** Illustrations of the pneumatic concentric nebulizers operating under the same experimental conditions.

lower than 100%. A cluster analysis of the critical dimensions of the nebulizers was performed and results clearly establishe two groups of nebulizers. The first group includes the SSN, CN and AN (*i.e.*, nebulizers with aerosol yields of 100%) and the second group is formed by the EN and SN (*i.e*, those with aerosol yields of lower than 100%). Trying to understand which of these dimensions determine the aerosol yield, a detailed examination of the data shown in Table 2 is required. Nevertheless, a few conclusions can be directly drawn: the EN provides a lower aerosol yield than the AN (43% and 100%, respectively) in spite of the fact that these are the nebulizers that have the lowest and highest $A_g$ value, respectively. Therefore, the aerosol yield does not seem to be related to $A_g$. However, with regard to the recessed area of the liquid capillary (dimension c), EN and SN show the highest value of this parameter and this seems to be the controlling factor in the aerosol yield. To get more information, a detailed cluster analysis of the variables was performed. Results indicate that the recessed area and inner diameter of the liquid capillary are the most influential parameters, which simultaneously affect the amount of solution that is converted into an aerosol.

**Aerosol cone angle.** Another characteristic of the primary aerosol that can affect its transport along the spray chamber is the aerosol cone angle.[24] A large cone angle contributes to the increase in the amount of aerosol that impacts against the side walls of the spray chamber.

Fig. 3 shows the differences in cone angles of the aerosols generated by the different nebulizers. Fig. 4 shows a section of the cone of aerosols generated by the nebulizers evaluated. As can be seen, the VGN is the nebulizer that generates the widest aerosol cones. The EN and SSN generate aerosols with similar cone angles, with those of the SSN being slightly sharper.

## Transport parameters

Fig. 5 shows the effect of the salt concentration of the sample on the solvent, $S_{tot}$, (Fig. 5a) and the analyte transport rate, $W_{tot}$, (Fig. 5b) for the three nebulizers tested. Data in Fig. 5 show that there is no noticeable effect of the salt concentration on either $S_{tot}$ or on $W_{tot}$. This behaviour is to be expected taking into account that, irrespective of the nebulizer used, there is almost no effect of the salt concentration on the pDSD (Fig. 2). Nonetheless, a reduction in the mass transport efficiency due to the presence of sodium chloride in the solution was reported by O'Hanlon *et al.* using a pneumatic nebulizer coupled to a double pass spray chamber.[25] It is worth noting that results in Fig. 5 were obtained using a cyclonic spray chamber. It is recognised that the effect of the inorganic acids and dissolved salts on the aerosol transport extent with respect to water is reduced when using a cyclonic spray chamber.[8]

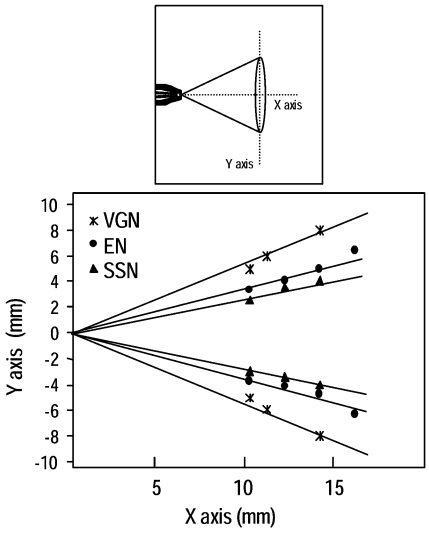


**Fig. 4** Aerosol cones generated by the nebulizers tested.

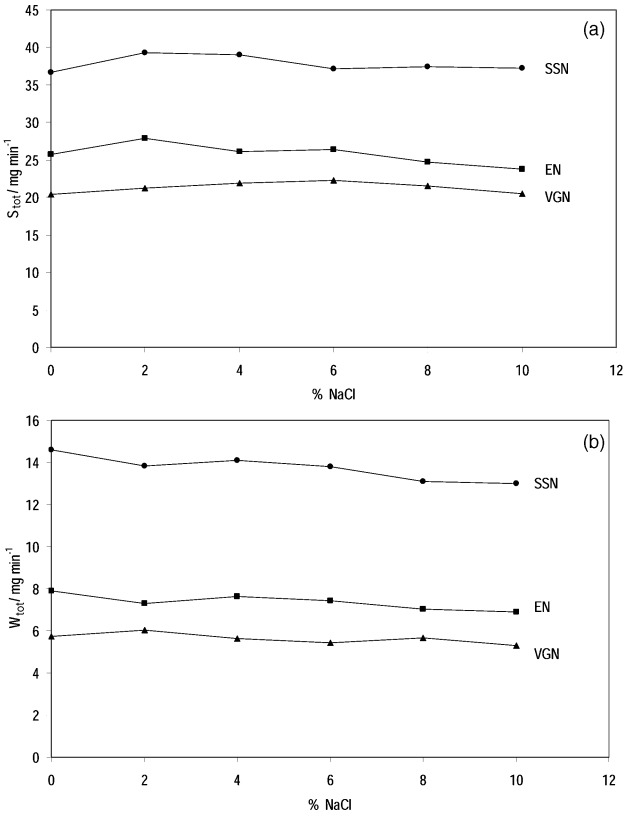


**Fig. 5** Effect of the sodium chloride concentration on the solvent, $S_{tot}$, (a) and analyte, transport rate, $W_{tot}$, (b) for all the nebulizers tested.

Comparing the relative behaviour of the different nebulizers, Fig 5 reveals that the SSN is the nebulizer that gives rise to the highest transport parameters. This is a direct consequence of the finest aerosols generated with the SSN. The EN gives rise to higher $S_{tot}$ and $W_{tot}$ values than the VGN, in spite of the fact that the latter nebulizer produces finer primary aerosols and a higher nebulization yield than the former. This apparently anomalous behaviour can be explained by considering the aerosol cone widths and the dimensions and position of the nebulizer inside the cyclonic spray chamber. Fig. 6 shows an outline of the nebulizer position inside the spray chamber. It can be observed that the VGN tip is recessed in the spray chamber with respect to the EN tip. This fact, together with the widest aerosol cone generated by the VGN, makes the fraction of the aerosol generated by the VGN that impacts against the inner walls of the spray chamber higher than that generated by the EN. As a consequence, and contrary to what is expected from their respective pDSD, the transport parameters obtained with the VGN are lower than those with the EN.

## Tertiary aerosol drop size distribution

Fig. 7 shows the effect of the sodium chloride concentration on the Sauter mean diameter of the tertiary aerosol ($tD_{3,2}$). These results reveal that, for all the nebulizers (in contrast to that observed for $pD_{3,2}$) $tD_{3,2}$ suddenly decreases on switching from pure water to 2% sodium chloride. Similar findings have been previously reported with both acid[26,27] and salt solutions.[28] However, for solution salt concentrations higher than 2%, this variable does not have a noticeable effect on the $tD_{3,2}$ values, irrespective of the nebulizer tested.

Another parameter that can be used to characterise the

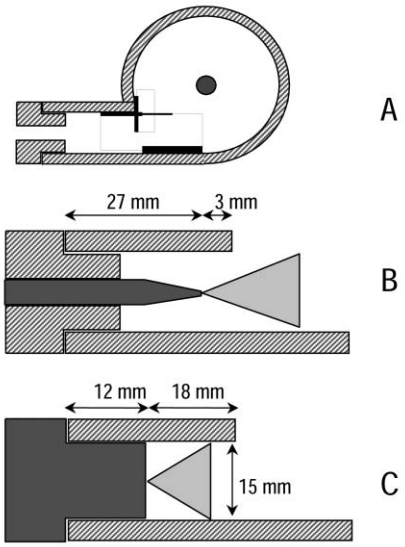


**Fig. 6** Scheme of the (A) cyclonic spray chamber and position of the nebulizer tips; (B) SSN and EN; and (C) VGN.

tDSD is the volume of tertiary aerosol contained in droplets with diameters below the lower limit of measurement of the instrument, *i.e.*, 1.2 μm ($tV_{1.2}$). It has been observed that, for all the nebulizers tested, $tV_{1.2}$ increases when switching from water to 2% sodium chloride. Further increases in the salt concentration do not affect the value of this parameter.

The above results demonstrate that the presence of salt clearly modifies the aerosol transport process, giving rise to a finer aerosol at the exit of the spray chamber, while the transport parameters remain unaffected (Fig. 5). This behaviour is not easy to explain and has been related to an ionic redistribution in the droplets.[27–29]

Attempting to explain the effect of the sodium chloride on the tDSD, the dependence of the characteristics of the tertiary aerosols on the pDSD and on the design of the spray chamber must be considered. Both factors, together with the physical properties of the solutions, such as density and volatility, determine the processes affecting the droplets during their transport to the atomization cell.[30–32] Since there is no effect of the salt concentration on the characteristics of the primary aerosols (Fig. 2), no changes in droplet collision and coagulation are expected. Moreover, solution density does not significantly change due to the presence of sodium chloride (Table 1). Therefore, modification of the droplet inertial deposition on walls and gravitational settlings should not be produced. Nonetheless, two differences appear when comparing water with sodium chloride aerosols that may explain the interference effect of sodium on the tDSD. Firstly, the presence of charged species in an aerosol droplet produces repulsion forces that can result in a droplet break-up, thus giving rise to finer droplets.[33,34] This fact could explain the lower $tD_{3,2}$ provided by the sodium chloride solutions. Secondly, it must be considered that evaporation of pure water aerosols is more severe than sodium chloride aerosols. Cresser and Browner demonstrated that, when nebulizing sodium chloride solutions of concentrations over 1%, evaporation effects on droplets of diameters greater than 0.5 μm are negligible.[35] For a monodisperse aerosol, evaporation will result in a decrease in the droplet diameter. For a polydisperse aerosol, this relationship is not so evident, since the solvent evaporation rate is higher for the smallest droplets. This effect can cause the smallest droplets to reduce in size to a value below the lower limit of the instrument (*i.e.*, 1.2 μm), and thus to be undetected, giving rise to an apparent increase in $tD_{3,2}$ [36] and a decrease in $tV_{1.2}$.

Fig. 7 shows that, irrespective of the nebulizer, the $tD_{3,2}$ values for the sodium chloride solutions are around 30% lower than those obtained for pure water. These results suggest that the effect of sodium chloride on the characteristics of tDSD is independent of the nebulizer used. To verify this statement, the tDSD curves obtained for all three nebulizers with both water and 2% sodium chloride solutions must be considered. These results, shown in Fig. 8, confirm the above-mentioned conclusion, since a clear parallel relationship between the tDSD curves obtained with pure water and 2% sodium chloride can be observed.

As regards the relative behaviour of the different nebulizers tested, Figs. 7 and 8 reveal that, as expected from the pDSD, the SSN gives rise to aerosols with the lowest $tD_{3,2}$. The EN, however, gives rise to finer tertiary aerosols than those obtained with the VGN. Again, this behaviour can be explained by taking into account both the dimensions and relative position of the nebulizers inside the spray chamber and the primary aerosol cone widths. In all cases, the differences in $tD_{3,2}$ for the different nebulizers are lower than those for the $pD_{3,2}$. This is due to the filtering effect of the spray chamber.

## Analytical figures of merit

**Emission signal.** Fig. 9 shows the variation of the net emission intensity of Mn II (normalized) against the sodium chloride concentration. These results reveal that there is a depressive effect of the sodium chloride concentration on the emission signal. The Mn II signal drops about 15% when switching from water to 10% sodium chloride, irrespective of the nebulizer. This behaviour seems to be related to plasma phenomena, since transport parameters do not change when

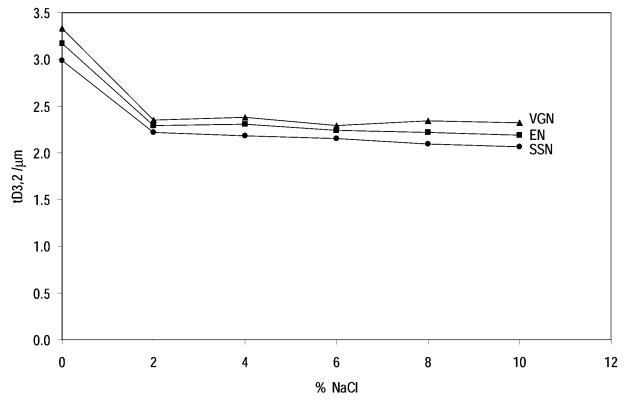


**Fig. 7** Effect of the sodium chloride concentration on the Sauter mean diameter of the tertiary aerosol, $tD_{3,2}$, for all the nebulizers tested.

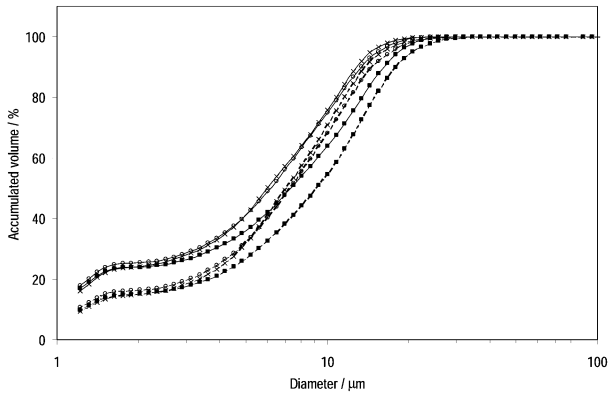


**Fig. 8** Volume drop size distribution of the tertiary aerosol obtained for pure water (dotted lines) and 2% sodium (continuous lines) with the nebulizers evaluated: (○) SSN; (X) EN; and (■) VGN.

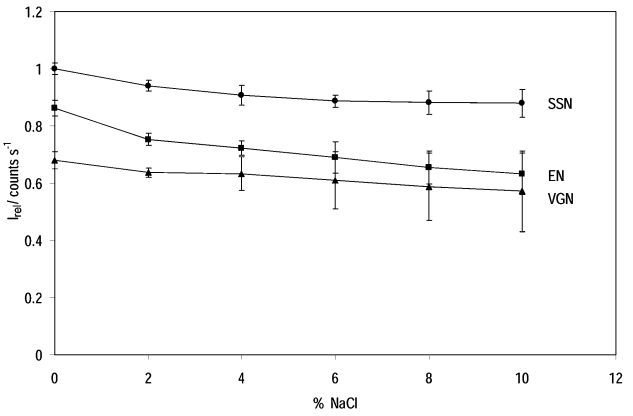


**Fig. 9** Effect of the sodium chloride concentration on the manganese emission intensity for all the nebulizers tested. [Mn] = 1 μg mL$^{-1}$.

the salt concentration is increased (Fig. 5). Nevertheless, for a given nebulizer, neither the Mg II/I nor the Cr II/I line ratios significantly change when the sodium concentration is increased. This confirms the robustness of the plasma conditions used with respect to matrix effects.[37–39] Similar findings have been previously reported in the literature.[40] A possible explanation for the change in the signal could be related to the formation of small salt deposits in the injector tube.

Regarding the relative behaviour of the nebulizers, Fig. 9 shows that the highest Mn II emission signals are obtained with the SSN followed by the EN and the VGN. This behaviour is to be expected taking into account their respective transport parameters (Fig. 5).

The effect of sodium chloride on the emission signal was also studied for different elements and lines. Fig. 10 gathers the results obtained for all the nebulizers evaluated. In this figure two different behaviours can be observed as a function of the nebulizer considered. For the SSN, results in Fig. 10a reveal that the effect of the sodium concentration on the emission signal is line-dependent. Thus, for the atomic lines studied, $I_{rel}$ steadily decreases as the salt concentration is increased. The magnitude of this detrimental effect ranges between 10% (for Cd 214.438) and 25% (for Ni 221.647 and Ba 455.403). For the ionic lines, $I_{rel}$ increases (Zn 213.856) or reaches a minimum and then increases. When switching from water to 10% sodium chloride, the emission signal changes from 110% for Zn 213.856 to up to about 70% for Cr 357.869. The behaviour of the SSN clearly indicates that non-robust conditions are used.[41] Thus, the values of Mg II/I ratios for this nebulizer range between 2.9 and 2.7 for water and 10% NaCl, respectively. For the remaining nebulizers, this ratio takes values of around 5.0. These results can be explained by taking into account that the SSN is the nebulizer that gives rise to the highest $S_{tot}$ (Fig. 5a). For the EN (Fig. 10b) and VGN (Fig. 10c), irrespective of the line tested, $I_{rel}$ steadily decreases as the salt concentration of the solution is increased. In these cases, when switching from water to 10% sodium chloride, the signal drops by 20% to 30% and by 5% to 15% for the EN and VGN, respectively. These results agree with the higher $S_{tot}$ values afforded by the EN. Finally, from Fig. 10, the behaviour of $I_{rel}$ does not seem to be related to $E_{sum}$ for any of the nebulizers.

**Precision.** Signal precision depends on the solution and nebulizer used. For a given nebulizer, an increase in the solution salt concentration causes a detrimental effect on the precision (*i.e.*, on the relative standard deviation, RSD) of the signal. Thus, for the SSN, the RSD ranges between 1% (for pure water or 2% NaCl) and 3% (for 10% NaCl). For a given

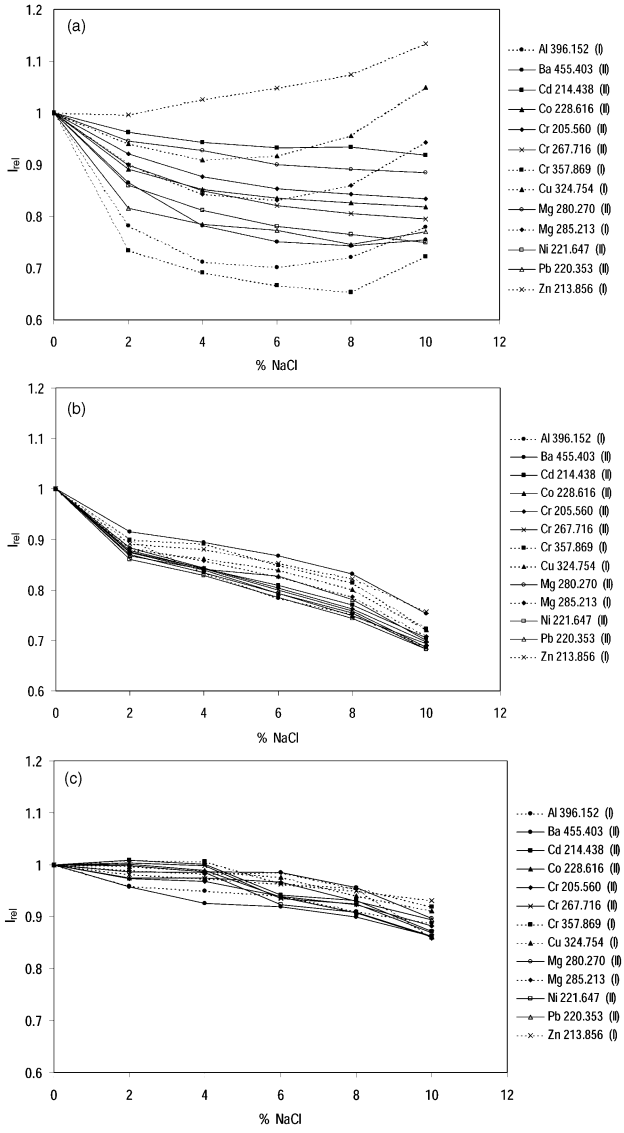


**Fig. 10** Effect of the sodium chloride concentration on the net emission intensity relative to water for the different lines and nebulizers tested: SSN (a); EN (b) and VGN (c).

NaCl concentration, the SSN is the best nebulizer in terms of signal precision, whereas the VGN is the worst. Thus, using 10% NaCl solutions, RSD values of around 3%, 6% and 12% for SSN, EN and VGN, respectively, are obtained.

**Limits of detection.** Fig. 11 shows the effect of the sodium concentration on the limits of detection (LOD) obtained with the SSN for different elements. In this study, LOD values were calculated according to the $3s_b$ criterion, where $s_b$ is the standard deviation of 20 replicates of the background. As can be seen in Fig. 11, an increase in the sodium chloride concentration gives rise to an increase in the LOD for all the elements tested. The deterioration factor lies between 1.6 (for Cr) and 7.2 (for Ba). This detrimental effect was observed for all the nebulizers tested and can be explained by taking into account the depressive effect of the sodium chloride concentration on both the emission signal (Figs. 9 and 10) and stability.

As regards the relative behaviour of the nebulizers tested, Table 5 shows the LOD obtained with the SSN and EN relative to those with the VGN for different elements and sodium chloride concentrations (2% and 10%). From these results it can be concluded that, in general terms, the SSN gives rise to the lowest LOD followed by the EN and the VGN. In this table

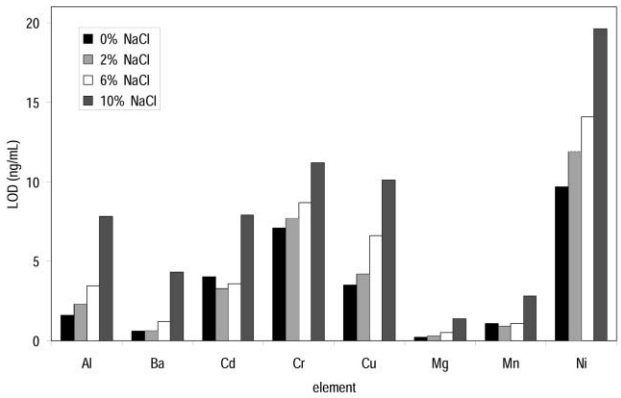


**Fig. 11** Effect of the sodium chloride concentration on the LOD obtained for some elements. Nebulizer: SSN.

**Table 5** Limits of detection obtained with the nebulizers tested

| | $LOD_{VGN}/LOD_{SSN}$ | | $LOD_{VGN}/LOD_{EN}$ | |
|---|---|---|---|---|
| Element | 2% NaCl | 10% NaCl | 2% NaCl | 10% NaCl |
| Al | 0.9 | 1.9 | 0.8 | 3.2 |
| Ba | 0.8 | 2.2 | 0.8 | 3.1 |
| Cd | 1.6 | 2.5 | 1.0 | 2.1 |
| Cr | 2.0 | 2.5 | 1.3 | 1.9 |
| Cu | 1.0 | 2.8 | 1.0 | 2.5 |
| Mg | 1.7 | 3.2 | 1.7 | 2.3 |
| Mn | 2.2 | 3.4 | 1.5 | 1.9 |
| Ni | 2.0 | 2.9 | 1.6 | 1.8 |

it can also be observed that the highest $LOD_{rel}$ values are obtained at the highest sodium concentration (*i.e.*, 10% sodium chloride). These results agree with the respective signals (Fig. 9) and stabilities.

## Conclusions

The use of pneumatic concentric nebulizers is a good choice for the elemental analysis of high salt content solutions by ICP-AES. Appropriate selection of the nebulizer makes it possible to directly analyse solutions of up to 10% sodium chloride without any clogging problems. Nebulizers must be selected by attending to the critical dimensions (*i.e.*, gas outlet section area, distance between liquid capillary and gas outlet, liquid capillary inner diameter and wall thickness). All these dimensions determine the fineness of the aerosols and the nebulization yield. These aerosol characteristics, in addition to the aerosol cone angle and position of the nebulizer inside the spray chamber, determine the transport of solution to the plasma.

Results shown in the present work clearly demonstrate that the interference effect of the sodium chloride in ICP-AES strongly depends on the nebulizer used. Among the concentric nebulizers tested, the SSN generates the highest interferences since it gives rise to the highest amount of solution transported to the plasma.

## Acknowledgement

The authors thank Mr. Alan Eastgate (Glass Expansion Europe, Switzerland) for the loan of the nebulizers and spray chamber.

## References

1 R. I. Botto, *Spectrochim. Acta, Part B*, 1985, **40**, 397–412.
2 G. M. Hieftje, P. J. Galley, M. Glick and D. S. Hanselman, *J. Anal. At. Spectrom.*, 1992, **7**, 69–73.
3 J. L. Todolí and J. M. Mermet, *Spectrochim. Acta, Part B*, 1999, **54**, 895.
4 M. Marichy, M. Mermet and J. M. Mermet, *Spectrochim. Acta, Part B*, 1990, **45**, 1195–1201.
5 M. Wu and G. M. Hieftje, *Spectrochim. Acta, Part B*, 1994, **49**, 149–161.
6 P. J. Galley and G. M. Hieftje, *Spectrochim. Acta, Part B*, 1994, **49**, 703–724.
7 M. T. C. de Loos-Vollebregt, R. Peng and J. J. Tiggelman, *J. Anal. At. Spectrom.*, 1991, **6**, 165–168.
8 S. Maestre, J. Mora, J. L. Todolí and A. Canals, *J. Anal. At. Spectrom.*, 1999, **14**, 61.
9 J. L Todolí, S. Maestre, J. Mora, A. Canals and V. Hernandis, *Fresenius' J. Anal. Chem.*, 2000, **368**, 773.
10 J. M. Mermet, *J. Anal. At. Spectrom.*, 1998, **13**, 419.
11 J. L. Todolí and J. M. Mermet, *J. Anal. At. Spectrom.*, 2000, **15**, 863.
12 J. Sneddon, *Sample introduction in atomic sepctroscopy*, Elsevier, Amsterdam, 1990.
13 B. Thelin, *Analyst*, 1981, **106**, 54.
14 R. F. Suddendorf and K. W. Boyer, *Anal. Chem.*, 1978, **50**, 1769.
15 T. T. Smith and M. B. Denton, *Appl. Spectrosc.*, 1990, **44**, 21.
16 B. L. Sharp, *J. Anal. At. Spectrom.*, 1988, **3**, 613.
17 C. Shuyin and L. Yunlong, *Spectrochim. Acta, Part B*, 1988, **43**, 287.
18 J. L. Todolí, A. Canals and V. Hernandis, *Spectrochim. Acta, Part B*, 1993, **48**, 1461.
19 L. Bordera, J. L. Todolí, J. Mora, A. Canals and V. Hernandis, 1998 Winter Conference on Plasma Spectrochemistry, Scottsdale, AZ, USA, January 5–10, 1998.
20 A. W. Adamson, *Physical Chemistry of Surfaces*, Interscience Publishers, New York, 1976, 3rd edn.
21 J. Mora, V. Hernandis and A. Canals, *J. Anal. At. Spectrom.*, 1991, **6**, 573.
22 B. A. Meinhard, D. K. Brown and J. E. Meinhard, *Appl. Spectrosc.*, 1992, **46**, 1134.
23 D. E. Nixon, *Spectrochim. Acta, Part B*, 1993, **48**, 447.
24 J. Mora, J. L. Todolí, A. Canals and V. Hernandis, *J. Anal. At. Spectrom.*, 1997, **12**, 445.
25 K. O'Hanlon, L. Ebdon and M. Foulkes, *J. Anal. At. Spectrom.*, 1997, **12**, 329.
26 I. I. Stewart and J. W. Olesik, *J. Anal. At. Spectrom.*, 1998, **13**, 1249.
27 J. L. Todolí, J. M. Mermet, A. Canals and V. Hernandis, *J. Anal. At. Spectrom.*, 1998, **13**, 55.
28 C. Dubuisson, E. Poussel, J. L. Todolí and J. M. Mermet, *Spectrochim. Acta, Part B*, 1998, **53**, 593.
29 J. A. Borowiec, A. W. Boorn, J. H. Dillard, M. S. Cresser, R. F. Browner and M. J. Matteson, *Anal. Chem.*, 1980, **52**, 1054.
30 W. C. Hinds, *Aerosol technology: properties, behaviour and measurement of airborne particles*, Wiley, New York, 1982.
31 B. L. Sharp, *J. Anal. At. Spectrom.*, 1988, **3**, 939.
32 R. F. Browner, A. W. Boorn and D. D. Smith, *Anal. Chem.*, 1982, **54**, 1411.
33 L. B. Loeb, *Static electrification*, Springer-Verlag, Berlín, 1958.
34 Q. Xu, G. Mattu and G. Agnes, *Appl. Spectrosc.*, 1999, **53**, 965.
35 M. S. Cresser and R. F. Browner, *Spectrochim. Acta, Part B*, 1980, **35**, 73.
36 J. Mora, A. Canals and V. Hernandis, *Spectrochim. Acta, Part B*, 1996, **51**, 1535.
37 J. M. Mermet, *Anal. Chim. Acta*, 1991, **250**, 85.
38 X. Romero, E. Poussel and J. M. Mermet, *Spectrochim. Acta, Part B*, 1997, **52**, 495.
39 E. H. van Veen and M. T. C. de Loos-Vollebregt, *J. Anal. At. Spectrom.*, 1999, **14**, 831.
40 C. Dubuisson, E. Poussel and J. M. Mermet, *J. Anal. At. Spectrom.*, 1998, **13**, 1265.
41 X. Romero, E. Poussel and J. M. Mermet, *Spectrochim. Acta, Part B*, 1997, **52**, 487.